ORIGINAL PAPER

Peptide gelation contributes to the tenderness and viscoelasticity of candy abalone

Yaxian Mo[1] · Jiaqi Ma[1] · Xinyu Zhang[1] · Guanghua Zhao[1] · Jiachen Zang[1] ✆

Abstract

Dried abalones are precious products, in which candy abalone is the most treasured one, owing to its unique taste. After rehydration and simmering, the core part tastes extraordinarily tender and viscoelastic, just like a soft candy which may almost melt in mouth. However, the reason for this has yet to be elucidated. The purpose of this study is to research the formation mechanism of the candy-like core in candy abalone. First of all, we characterized the viscoelasticity, microstructure and protein changes of candy abalone during the simmering process. The texture results indicated that the springiness and adhesiveness of candy abalone showed an increase. Scanning and transmission electron microscopy suggested that myofibrillar protein in candy abalone formed a dense three-dimensional network hydrogel structure. Sodium dodecyl sulfate–polyacrylamide gel electrophoresis revealed such a hydrogel structure might be derived from the degradation of the myofibrillar protein during the drying process. Also, we identified degraded peptides mainly stemmed from paramyosin by mass spectrometry. Moreover, molecular dynamics simulation revealed that the hydrogen bonds and hydrophobic interactions are mainly responsible for the self-assembly of peptides during the rehydration and simmering stages. Different from reported protein hydrogels, the rheological and morphological properties of the formed peptide hydrogels in candy abalone have significant changes. In this study, we found that the myofibrillar protein of fresh abalone degraded into peptides during the drying process, which further cross-linked to form a peptide hydrogel during the rehydration and simmering stages, thereby producing a unique viscoelastic candy-like core in candy abalone.

✉ Jiachen Zang
zangjiachen@cau.edu.cn

1   College of Food Science and Nutritional Engineering, China
     Agricultural University, Beijing 100083, China

Graphical abstract
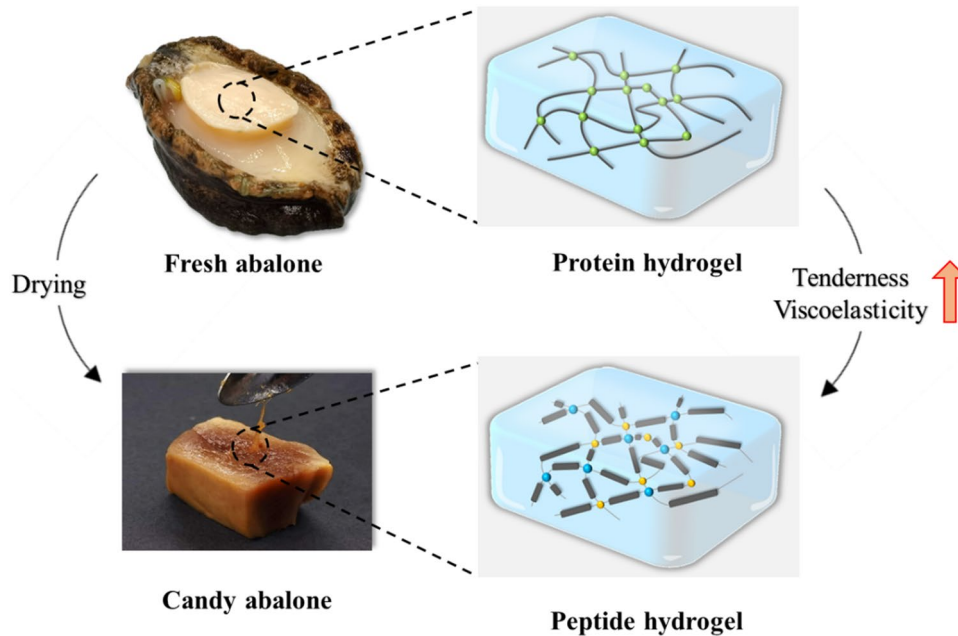
Introduction

Abalone, a typical marine shellfish, has been regarded as a great delicacy ever since ancient times in Asian countries, owing to its unique taste. In the last 40 years, advanced cultivating technique has increased the global production of abalone fivefold, reaching 22,000 tons in 2020 [1]. Abalone is rich in a series of nutrients such as essential amino acids, bioactive peptides, long-chain polyunsaturated fatty acids, vitamins, and minerals [2, 3]. Thus, abalone can be a source of bioactive substances with anti-thrombotic, anti-coagulant, anti-inflammatory, and antioxidant activities [1].Besides, the abalone provides plenty source of bioavailable proteins, mainly including myofibrillar proteins and collagens. These two types of proteins not only support the nutritional value, but also play key roles in the textural characteristics of abalone [3].

Besides fresh consumption, a great number of abalones are processed into canned, frozen, and dried products to avoid spoilage and develop organoleptic properties of abalones [4]. Therein, dried abalone has a long history, in which candy abalone is the most popular product due to its excellent taste. After rehydration and simmering, the core part of candy abalone, namely the adductor muscle, tastes extraordinarily tender and sticky, just like a soft candy that may almost melt in the mouth. It is also one of the most expensive foods, because of the rare source and complicated

preparation. Firstly, the size of the abalone is a prerequisite for the formation of candy abalone, in which bigger abalones are preferred to be chosen. Secondly, it is a long processing process for candy abalone, including cleaning, pickling, boiling, drying, and rehydrating. Then the cooking of candy abalone is also of great essence for its organoleptic characteristics, in which long-time simmering is necessary. As the physical and chemical properties, especially the tissue structures of candy abalone, undergo significant changes during preparation, the adductor muscle exhibits a soft, chewy and viscoelastic texture in the mouth after cooking, which is considerably different from dishes made by fresh abalone. Thus, the formation of a candy-like core is considered to be the most typical characteristic of top dried abalone. However, the drying and simmering process of candy abalone is quite traditional and empirical, and has no theoretical or scientific basis yet.

Abalone muscle consists mainly of myofibrillar proteins (300–500 g.kg^{-1}), collagenous tissue protein (100–300 g. kg^{-1}), and some other water-soluble proteins (100–200 g. kg^{-1}) [5]. Heat treatment is commonly used to reduce microbial problems before the consumption of seafood while improving palatability. During heat treatment, the majority of proteins undergo denaturation, aggregation and gel formation, which lead to changes in microstructure and texture [6–8]. Myofibrillar protein is mainly found in the adductor muscle in the center of abalone, accounting for about 420 g.

kg^{-1} of the total protein [9]. Paramyosin is a vital myofibrillar protein in molluscan muscle. It is a kind of fibrous structural protein that accounts for 380–480 g.kg^{-1} of the myofibril [10]. It is highly conserved in structure and usually contains two identical subunits with a molecular weight of approximately 200 kDa. Besides, it has been shown that paramyosin is an α-helical fiber with a coiled-coil structure. On the one hand, paramyosin plays a key role in thick filament structure. On the other hand, it has been suggested that it is related to the maintenance of "catch" state [11]. In the "catch" state, the filaments made up of paramyosin fuse with each other, generating high tensions with low energy consumption [12]. It has been reported that some structural changes, such as modification of amino acid side chains, breakage and structural unfolding of peptide chains, protein degradation, and polymer generation, happen upon myofibrillar proteins along with heat processing [13–15]. Such structural changes in muscle proteins have a strong influence on the texture of abalone, which may be pivotal in the formation of candy-like core in dried abalone.

Gelation is a common behavior of myofibrillar protein, which is responsible for the cohesive structure and firm texture of abalone products [16]. It involves denaturation and irreversible aggregation of the protein, culminating in the formation of a three-dimensional network. Thermal treatment is generally applied to induce the gelation of myofibrillar proteins in aquatic animals [17, 18]. Besides processing temperature, pH is also a crucial factor for protein gelation. Le et al. compared abalone gels prepared at different pH [19]. In their report, a progressively denser network was observed in the gel with pH increasing, which may be caused by the changes in tertiary structure. In our recent work, a kind of sol–gel phase-reversible hydrogel has been constructed by paramyosin in the adductor muscle of abalone. Zinc ions play a key role in tuning the assembly and disassembly of paramyosin, during which process, the mechanical property changes. After the sol–gel transition, the mechanical strength showed a significant increase. Moreover, due to the highly conserved structure of natural paramyosin, the mechanical property of the paramyosin hydrogel could be fine-tuned by non-covalent interaction with small molecules [20]. It spired us that the unique property of candy abalone may be a result from the discrete assembly behavior of myofibrillar proteins within adductor muscles, compared with fresh abalones.

The purpose of this study is to investigate the characteristics of candy abalone on the one hand and to research the formation mechanism of the candy-like core during the simmering process on the other hand. Upon characterizing the viscoelastic, microstructure and protein changes of dried abalone during the simmering process, we identified the peptides in the candy abalone gel by mass spectrometry and studied the self-assembly feature of peptides. It was found that the unique taste of the candy abalone was most likely due to the degradation of paramyosin into peptides during the drying process, which were further cross-linked to form a peptide gel in the following process of rehydration and simmering, as shown in Fig. 1. This study reveals the scientific mechanism of the formation of candy abalone, which also enhances our understanding of how gelation affects the texture of foods.

Materials and methods

Materials and reagents

Dried abalones (Kippin Abalone) were imported from Japan and purchased on the market. Fresh abalones (*Haliotis discus hannai*) were purchased from the local market. The weight of a dried abalone was 10 ± 1 g (excluding the shell and viscera), and the fresh abalone was 32 ± 3 g (excluding the shell and viscera).

Glutaraldehyde ($C_5H_8O_2$), uranyl acetate ($C_4H_{10}O_8U$), sodium chloride (NaCl), tris (hydroxymethyl) aminomethane (Tris) and maleic acid ($C_4H_4O_4$) were obtained from Solarbio (Beijing, China). Sodium dodecyl sulfate (SDS), polyacrylamide, β-mercaptoethanol, bromophenol blue and Coomassie Brilliant Blue R-250 were acquired from Beijing Biodee Biotechnology Co., Ltd. (Beijing, China). Ethanol (CH_3CH_2OH), acetic acid (CH_3COOH) and urea (CH_4N_2O) were purchased from Lanyi Biotechnology Co., Ltd. (Beijing, China). All other chemicals and solvents were analytical grade or purer.

Preparation of candy abalone

The dried abalone was rehydrated in ultrapure water, and the ultrapure water was changed daily. The rehydration was completed after approximately 3 days and ready for use. The fresh abalone used as a control was shelled, rinsed with coarse salt and then placed in sodium chloride solution for 12 h at 4 °C. The abalones were taken out and washed to remove the black mucus on the surface. After that, the dried and fresh abalones were firstly boiled quickly on high heat until the water boiled and then simmered (90 °C) for 0 h, 5 h, 7.5 h and 10 h for the sampling of dried and fresh abalones respectively. After the preparation of the candy abalone, some of them were characterized. Other samples were stored at − 20 °C for further analysis.

Characterization of viscoelastic properties of candy abalone

Textural measurement

The textural properties were determined with reference to the following method [21]: the adductor muscles of dried and
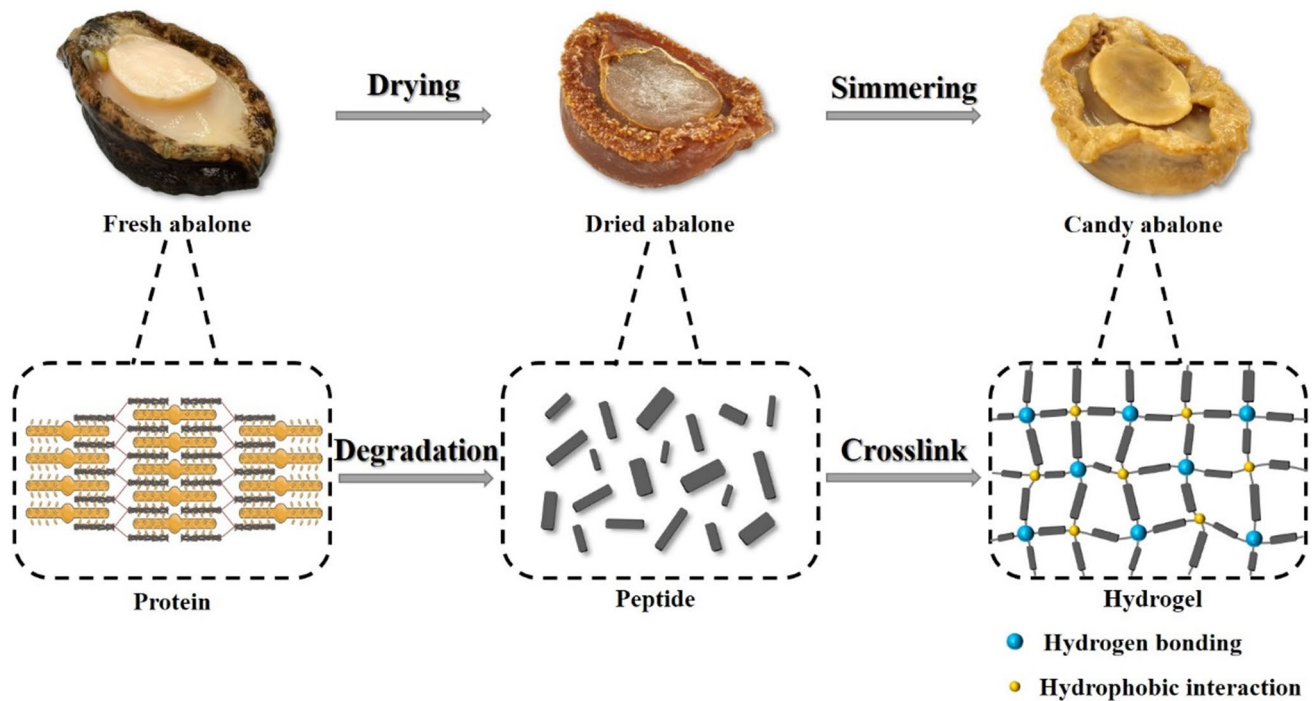
Fig. 1 Schematic diagram of the formation of tender and viscoelastic textural characteristics of candy abalone

fresh abalones were cut into rectangles of $30 \times 20 \times 20$ mm and then cut longitudinally in the middle, and next evaluated for hardness, springiness, adhesiveness and chewiness of candy abalone and fresh abalones along the vertical sections with a Texture Analyzer (TA-XT2i, Stable Micro Systems, Co., Ltd, UK). The measurement mode was selected as texture profile analysis (TPA). The measurement probe was a P/35 cylinder. The equipment was set as follows: pre-test speed, test speed and post-test speed were all of 1.0 mm/s, compression degree of 15%, and trigger force of 5 g. Each sample underwent 2 cycles of compression analysis, with a 5 s relaxation time between the 2 cycles. Each group of samples was measured in three parallels, and each parallel was repeated twice.

Rheology test

The adductor muscles of candy abalone at 0, 5, 7.5 and 10 h were mixed with deionized water (w: $v = 1:1$) and then homogenized with a homogenizer, and fresh abalone at the above-mentioned different times were used as controls. The oscillatory rheology of abalone homogenate was carried out on a rotated rheometer (DHR TA Instrument) equipped with a parallel steel plate (40 mm diameter). The strain oscillation scans were performed at 1 Hz where a continuous change of the oscillatory strain between 0.1–1000% at 25 °C. The gap of the tests was 100 μm. The dynamic frequency sweep was carried out at 1% strain, and the frequency was between 0.1 and 100 Hz.

Scanning electron microscopy (SEM)

Sample preparation for SEM observation was performed according to the method of Urbonaite et al. [22] with slight modifications. Briefly, the adductor muscles of dried and fresh abalones were cut into $3 \times 2 \times 1$ mm rectangles and prepared in 1.5 mL Eppendorf tubes. They were then immersed in 0.1 M phosphate buffer (pH = 7.4) containing 2.5% (v/v) glutaraldehyde at 4 °C overnight, followed by three washes with 0.1 M phosphate buffer (pH = 7.4). Then, the samples were dehydrated twice in ethanol with serial concentrations of 25%, 50%, 70%, 85%, 95% and 100% (v/v), with each concentration lasting for 15 min. After dehydration, the samples were dried at the critical point using CO_2 as a transition fluid. Finally, the samples were mounted on SEM stubs, coated with gold and observed at an accelerating voltage of 3 kV (SU8020, Hitachi, Tokyo, Japan).

Transmission electron microscopy (TEM)

A volume of 10 μL filaments from the center of abalone adductor muscles dispersed in deionized water was deposited on a carbon-coated copper grid for 5 min incubation. The excess solution was then carefully removed with filter paper and stained with 2% uranyl acetate for 5 min. After

the removal of the excess staining solution, the copper grids were air-dried under light conditions for at least 30 min. Transmission electron micrographs were imaged with a Hitachi H-7650 transmission electron microscope at 80 kV.

Protein extraction and sodium dodecyl sulfate–polyacrylamide gel electrophoresis (SDS-PAGE)

The extraction method of proteins from candy and fresh abalones were mainly based on the method described by Tadpitchayangkoon et al.[23] with slight modifications. The adductor muscle (2 g) of abalone was minced and mixed with 30 mL cold deionized water. The mixture was then homogenized at $3200 \times g$ for 2 min. To avoid overheating, the sample was placed on ice and homogenized intermittently (30 s followed by a 10 s rest interval). After centrifugation at $10,600 \times g$ for 15 min, the supernatant and precipitate were collected separately. Then, 30 mL of NaCl (3 g. kg^{-1}) was added to the precipitate, and the above steps were repeated to collect the precipitate. The supernatant of two centrifugations was combined as water-soluble protein. The precipitate was added to 30 mL of cold 0.6 M NaCl-20 mM Tris-maleic acid buffer (pH = 7.0), homogenized at $3200 \times g$ for 1 min, and the protein was solubilized overnight at 4 °C. After centrifugation at $10,600 \times g$ for 15 min, the supernatant was collected as salt-soluble protein and precipitate as insoluble protein.

SDS-PAGE was performed with 5% stacking gel and 15% separating gel according to the method of Laemmli [24]. The volume ratio of sample-to-buffer was 1:1. Each sample was heated at 100 °C for 5 min. Electrophoresis was carried out at 180 V for approximately 45 min. Afterward, the gels were stained with Coomassie Brilliant Blue R-250 and destained with deionized water, ethanol and acetic acid (6:3:1). A protein standard ranging from 10 to 100 kDa was used to estimate the molecular weight of the proteins.

Preparation and rheology test of dried abalone peptide gel

The rehydrated dried abalone was mixed with deionized water at 1:2 (w: v). Then it was homogenized by a homogenizer at $2200 \times g$ for 2 min (30 s followed by a 10 s rest interval), the same procedure for fresh abalone as a control. The mixtures were adjusted to the target pH values (5.0 to 7.0) using 0.5 M HCl or NaOH. Afterward, they were heated in a water bath from 25 to 80 °C at 1.5 °C/min increments and held at 80 °C for 20, 40 and 120 min. Next, they were immediately cooled with ice water and stored at 4 °C overnight before the rheology test. Then, the effect of different concentrations (w: v = 1:1, 1:2 and 1:4) on the rheological properties of gels formed by self-assembly of peptides derived from dried abalone was investigated based on the

above experiments to derive heating time for the maximum of G' and G".

The oscillatory rheology of abalone homogenates was carried out on a rotated rheometer (DHR TA Instrument) with a parallel steel plate (40 mm diameter). The strain oscillation scans were performed at 1 Hz, where a continuous change of the oscillatory strain between 0.1 and 3000% at 25 °C. The gap of the tests was 100 μm.

Identification and analysis of possible peptides in candy abalone

The insoluble protein in 2.6 was solubilized with 8 M urea (w: v = 3:20) and stirred overnight at 4 °C. After centrifugation at $10,600 \times g$ for 30 min, the supernatant was aspirated. It was transferred to a 10 kDa ultrafiltration tube to remove proteins larger than 10 kDa. Then the filtered solution was sent to the Protein Research and Technology Center, Tsinghua University (Beijing, China) for sequencing.

Molecular dynamics (MD) simulation

The molecular dynamics simulation was performed using GROMACS. The minimum distance between any solute and the edge of the periodic box was 1.0 nm. The box was filled with extended single-point charge water molecules and a solvation system. And then, adding counter ions to neutralize the overall charge of the complex. After minimizing the energy, the system was balanced in two steps: firstly, canonical ensemble (NVT, 0.1 ns) and secondly, isothermal isobaric (NPT, 0.1 ns). Finally, 250 ns MD simulation was performed at 1 bar and 300 K, and the atomic coordinates were recorded in the trajectory file at every 0.2 ps. Subsequently, the molecular dynamics simulation results were analyzed using GROMACS (version 19.5).

Statistical analysis

All results were expressed as mean values ± standard deviation (SD) from three independent measurements. One-way analysis of variance (ANOVA) of the data was conducted using IBM SPSS Statistics 26.0. The Tukey's test or unpaired t-test was used, with a P-value < 0.05 considered statistically significant. Furthermore, Origin 8.0 was used for graphing.

Results and discussion

The textural characteristics of candy abalone

In terms of the edible quality of muscle foods, the texture is one of the most essential sensory attributes and

an important aspect in evaluating the quality of candy abalone. Various factors affect the texture changes, which can be mainly classified into physical, chemical and biological factors, among which the composition of protein, structural morphology of muscle fibers, moisture content and distribution are more influential. Generally, the texture can be measured by puncture, compression, shear and tension to obtain a force–deformation curve. The force values, deformation, slope and peak area shown in the curve are calculated as texture indicators. At present, the TPA mode is the most commonly used method to determine the quality of aquatic products, and it is a double-compression determination mode. Thus, the results are more accurate and reliable.

The value of hardness was the maximum peak at the first compression. The changes in the hardness of the adductor muscle of candy and fresh abalones with simmering time are shown in Fig. 2a. Overall, the hardness of candy abalone showed a decrease after 10 h of simmering, with a decrease of 15% and a hardness value of only 7.05 N. The hardness of the fresh abalone served as a control, had an initial hardness value of 5.25 N, lower than the candy abalone. The hardness of the fresh abalone decreased with increasing simmering time ($P < 0.05$). It has been shown that there was a strong relationship between the hardness of abalone muscle and collagen [5, 25]. The decrease in hardness of candy and fresh abalones was probably due to the change in collagen structure during heating, which
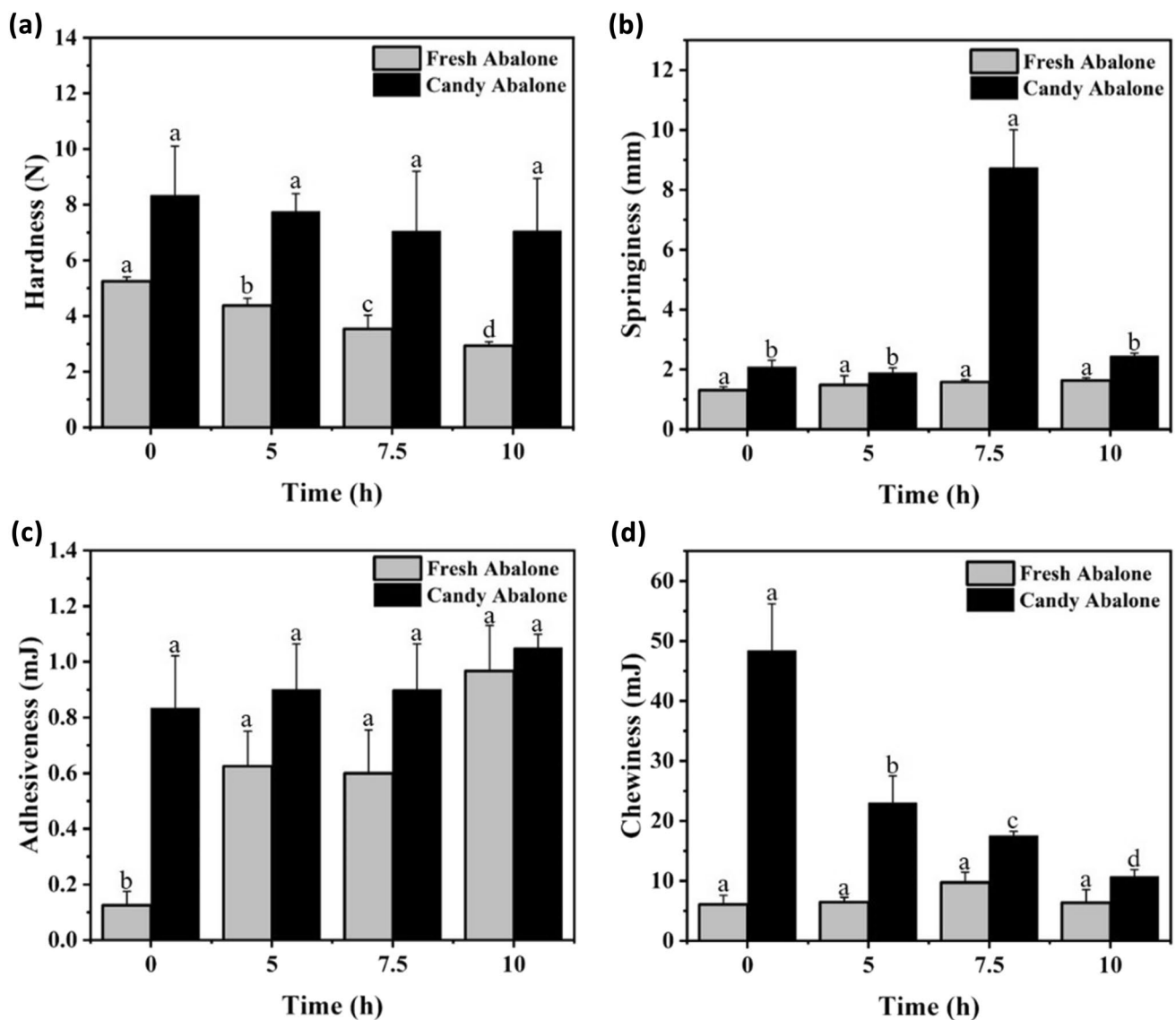

Fig. 2 The textural changes of candy and fresh abalones under different simmering times. **a** The changes of hardness. **b** The changes of springiness. **c** The changes of adhesiveness. **d** The changes of chewiness. Different small letters mean significant differences ($P < 0.05$)

caused some collagen to be converted into soluble gelatin, resulting in increased solubility and loosening of muscle fibers. All through the heating process, the hardness of the candy abalone adductor muscle was higher than that of fresh abalone. On the one hand, this was due to the higher degree of aggregation and cross-linking of myofibrillar proteins in the candy abalone. On the other hand, during the simmering process, the protein underwent a carbonylation reaction, and the hydrophobicity of the protein surface increased. Also, the process tended to form disulfide bonds. The cross-linking formed by protein oxidation enhanced the structure of the myofibrillar protein of candy abalone, resulting in a greater hardness [26].

The springiness reflects the deformation of the food when an external force is applied and the degree of recovery after the force is removed [27]. As shown in Fig. 2b, candy abalone' s springiness showed a fluctuating increase after simmering for 7.5 h ($P < 0.05$), which increased by 310%. In contrast, during the simmering process, the elasticity of fresh abalone remained basically the same. Overall, the springiness of fresh abalone was significantly lower than the candy abalone ($P < 0.05$). Herrero et al. [28] showed that β-folding and turning were positively correlated with changes in hardness and springiness, while the specific gravity of α-helix was negatively correlated with changes in hardness and springiness. Therefore, this result suggests that the simmering process may cause changes in the secondary structure of the myofibrillar protein in the candy abalone, resulting in the unique elastic texture of candy abalone.

As shown in Fig. 2c and d, the adhesiveness and chewiness properties of candy abalone varied with simmering time increasing. The adhesiveness of candy abalone presented a slightly increase ($P > 0.05$) with increasing simmering time. Meanwhile, the adhesiveness property of fresh abalone showed a fluctuant increasing trend. Moreover, it was significantly different from the initial value after 5 h of simmering ($P < 0.05$). During the simmering process, the adhesiveness of candy abalone maintained higher than fresh abalone.

On the whole, the chewiness of candy abalone significantly decreased ($P < 0.05$), similar to the hardness trend. Therefore, there is a positive correlation between chewiness and hardness. Also, a study indicated that the decrease in chewiness might be caused by water loss and deterioration of muscle tissue [29]. However, the chewiness of fresh abalone slightly increased after 7.5 h of simmering ($P > 0.05$) and subsequently slightly declined. After boiling for 5 h, candy abalone was less likely to be chewed compared with fresh abalone. As the simmering time increased, the candy abalone became easier to chew. But the chewiness value of candy abalone was always greater than that of fresh abalone throughout the process.

The rheological characteristics of candy abalone

The rheological behavior can reflect the gel properties of candy abalone. On the one hand, it can quantitatively assess the mechanical properties of the candy abalone gel; on the other hand, it can also sensitively reflect the processes of sol–gel and gel-sol transformation. In amplitude oscillatory shear measurements, the storage modulus (G') and loss modulus (G″) are the critical hydrogel properties monitored according to time, frequency, and strain [30]. G' represents the deformation energy stored in the material during the shear test, which is the material's stiffness. G″ represents the energy dissipated of the material during shear, which is the flow or liquid-like response of the material. Therefore, we used the typical oscillatory shear rheology to characterize the rheological properties of candy and fresh abalones at different simmering times, as shown in Fig. 3. Strain-dependent oscillatory shear rheology of candy abalone and fresh abalone with a fixed frequency of 1 Hz were presented in Fig. 3a and b. The storage modulus (G') of candy abalone fluctuatingly decreased with increasing simmering time in the oscillatory strain range of 0.1%-1000%. The initial value of the G' of dried abalone was 2 times higher than its value after 10 h of simmering. This indicated the decrease in stiffness of the candy abalone, which was consistent with the texture analysis. The loss factor (tanδ) is the ratio of the loss modulus (G″) to the storage modulus (G″) of the sample. Loss factor is the ratio of the viscous and the elastic component in the dynamic deformation, showing the quotient of the lost and the stored deformation energy. The larger the loss factor indicates that the material is more viscous, and the smaller the loss factor indicates that the material is more elastic, which can indicate the state of the material within a certain range. The loss factor for candy and fresh abalone in the linear viscoelastic region at 1% strain was shown in Table 1. The loss factor of candy abalone kept small and increased slightly during the simmering process, which demonstrated that the energetic elastic behavior was more dominant in comparison to the viscous behavior in 1% strain. Meanwhile, the loss factor increased in candy abalone indicated that the more energy was dissipated after simmering for 10 h ($P < 0.05$), the more the solid-like character gradually decreased, and the lifetime of the gel network bonds were gradually shortened [31, 32]. Moreover, with the increase of oscillatory strain, the intersection of storage modulus and loss modulus appeared, indicating the disruption of the three-dimensional gel of the candy abalone, which transited to the sol state. The strain of its transition from gel-sol fluctuatingly decreased with the increase of simmering time, from 118 initially to 11% eventually, which explained the characteristic of the candy abalone that melted in the chewing process. In contrast, the
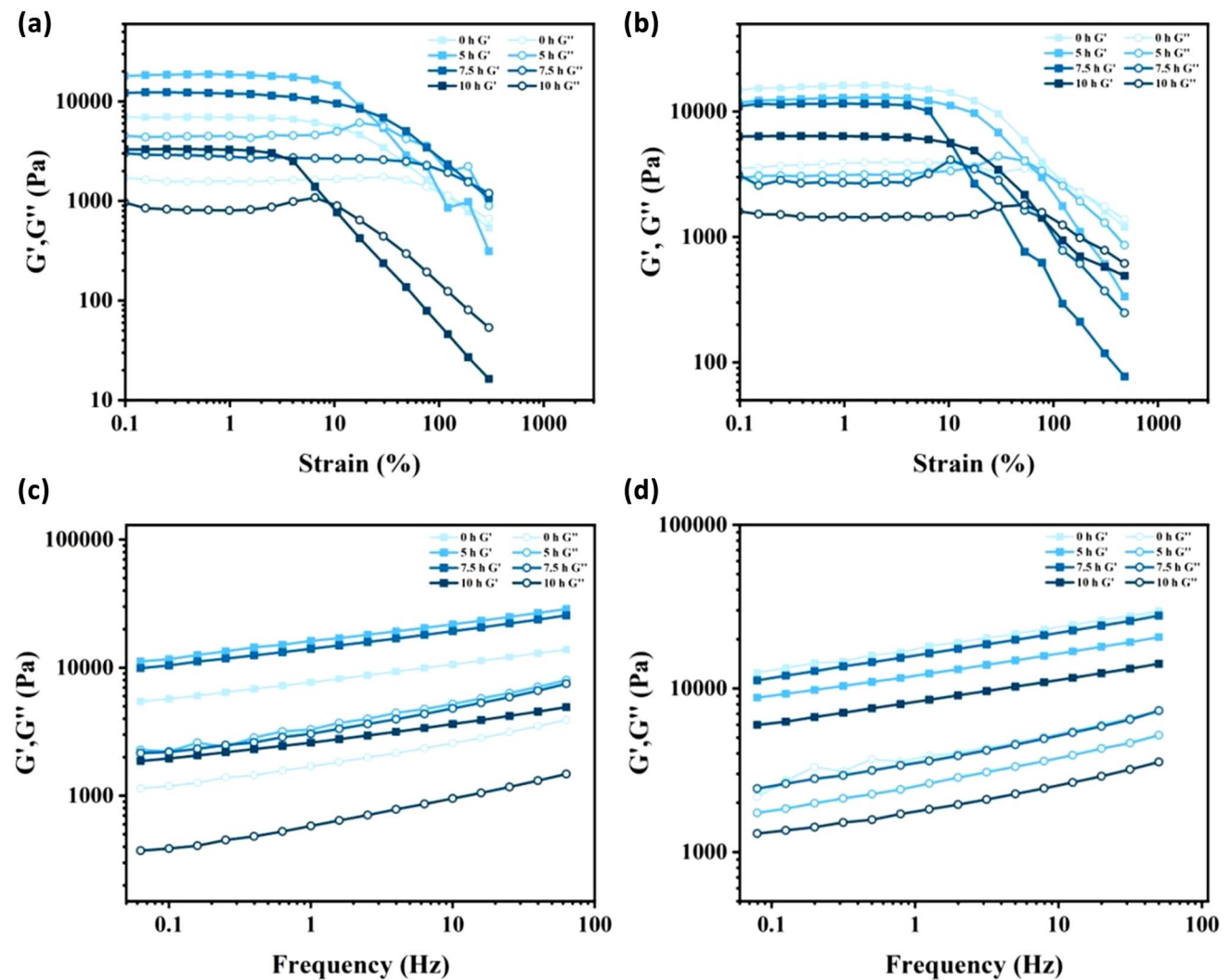
Fig. 3 Strain-dependent oscillatory shear rheology of **a** the candy abalone gel and **b** fresh abalone gel with a fixed frequency of 1 Hz at 25.0±0.1 °C. Dynamic frequency sweep rheology of **c** the candy abalone gel and **d** fresh abalone gel with a fixed strain of 1% at 25.0±0.1 °C

Table 1 Loss factor (tanδ) of candy and fresh abalone at different simmering times under 1% strain of oscillatory shear rheology and dynamic frequency sweep rheology at 1 Hz

Time (h)	Strain-dependent oscillatory shear rheology		Dynamic frequency sweep rheology	
	Candy abalone	Fresh abalone	Candy abalone	Fresh abalone
0	0.231 ± 0.001^b	0.240 ± 0.001^a	0.220 ± 0.003^a	0.215 ± 0.002^a
5	0.226 ± 0.006^b	0.240 ± 0.007^a	0.203 ± 0.001^b	0.208 ± 0.005^a
7.5	0.234 ± 0.001^b	0.234 ± 0.001^{ab}	0.217 ± 0.005^a	0.220 ± 0.003^a
10	0.245 ± 0.001^a	0.231 ± 0.005^b	0.224 ± 0.002^a	0.214 ± 0.002^a

Different letters in each column mean significant differences ($P < 0.05$)

storage modulus of fresh abalone mildly decreased after 7.5 h of simmering, and a significant decrease occurred after 10 h of simmering. The strain of gel-sol transition gradually decreased after 7.5 h of simmering, which may be related to the decrease in hardness and storage modulus of fresh abalone. In general, the dynamic frequency sweep suggested that both G′ and G″ depended slightly on frequency while the gel state remained at various frequencies (Fig. 3c and d). The loss factor remained small and steady at 1 Hz from Table 1, demonstrating the time-stability of the gel networks [33]. Although boiling might refold or denature the myofibrillar proteins, the rheological properties were steady in medium frequency, showing the high quality of the candy abalone gel.

The Changes in microstructure of candy abalone adductor muscle

The above experiments described the textural characteristics of simmered candy abalone. To get more detailed insights into the microstructures of the candy-like core, scanning electron micrographs were conducted to detect the adductor muscles of dried and fresh abalones at different simmering times. At low magnification, the three-dimensional morphology of the dried abalone surfaces gradually became inhomogeneous and rough as the simmering time increased. After 10 h of simmering, a dense gel network structure was formed. This may be due to the fact that the denaturation rate of myofibrillar proteins was higher than the aggregation rate during the simmering process, which resulted in a dense gel network of dried abalone after 10 h boiling [34]. Figure 4a, b, c and d show that the diameter of dried abalone myofibrils decreased slightly, and fibers began to generate around the myofibrils after 7.5 h (Fig. 4c and d). They cross-linked together in spherical aggregates. Thus, the network was denser in the small aggregation areas compared with the large aggregation areas. During the simmering process, the structures of the proteins gradually unfolded, and the internal hydrophobic groups were exposed, which increased the hydrophobic interactions of the proteins. At the same time, oxidation of the proteins led to the formation of disulfide bonds, which together caused aggregation and cross-linking of myofibril proteins. The muscle fiber diameter of fresh abalone gradually decreased, and the pore size also slightly decreased, but the changes were not obvious (Fig. 4e, f, g and h). Overall, the muscle fibers of fresh abalone did not change significantly during the simmering process.

It is a typical phenomenon that when the simmered candy abalone is cut, silk-like materials are easily observed adhering to the knife. While such a phenomenon may not appear on the fresh abalone after simmering treatment (Fig. S1). It corresponds to the above textural and rheological results. In order to further observe the microscopic morphology of the "silk", we conducted transmission electron microscopy with higher resolution, and the results are shown in Fig. 5. Before simmering, the dried abalone showed short and thin filaments with some cross-linking (Fig. 5a). After 5 h of simmering, the short and thin nanofibrils intertwined to form thicker nanofibrils (Fig. 5b). After 7.5 h of simmering, gelation further cross-linked the nanofibrils, resulting in a denser three-dimensional network structure (Fig. 5c). However, when the simmering time was further increased, the samples showed partial breakage of the cross-linked network and increased pore size (Fig. 5d). Overall, the dried abalone showed the best gelation state after 7.5 h of cooking, with dense and uniform characteristics. Nevertheless, fresh abalone initially displayed a small nanoparticles aggregate, eventually forming a large protein aggregate (Fig. 5e, f, g and h). Therefore, the formation of network structures observed by transmission electron microscopy could account for the tender and stickier properties of the candy abalone after simmering.

The changes of water-soluble proteins, salt-soluble proteins and precipitate on SDS-PAGE

In addition to water, protein occupies the highest content in the adductor muscle of the abalone. Therefore, the structural change of protein is an important reason for the "candy" formation. We used SDS-PAGE to investigate the protein changes of abalone after drying and simmering to study the forming mechanism of candy abalone. The abalone adductor muscle contains mainly water-soluble proteins, salt-soluble proteins and insoluble matrix proteins (collagen). Water-soluble proteins mainly include some enzymes related to
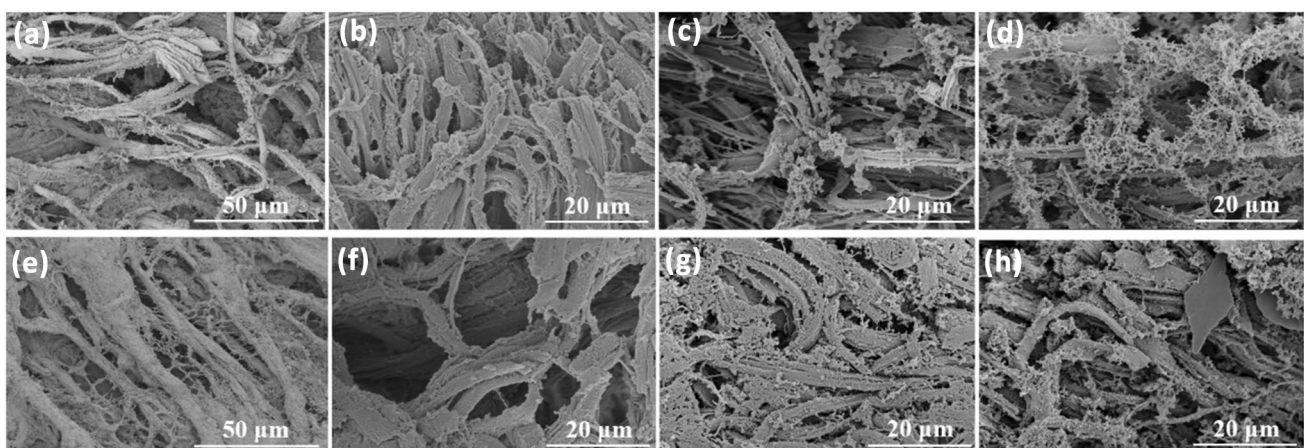

Fig. 4 Scanning electron micrographs of candy and fresh abalones under different simmering times. **a–d** Candy abalone simmered for 0, 5, 7.5 and 10 h. **e–h** Fresh abalone simmered for 0, 5, 7.5 and 10 h
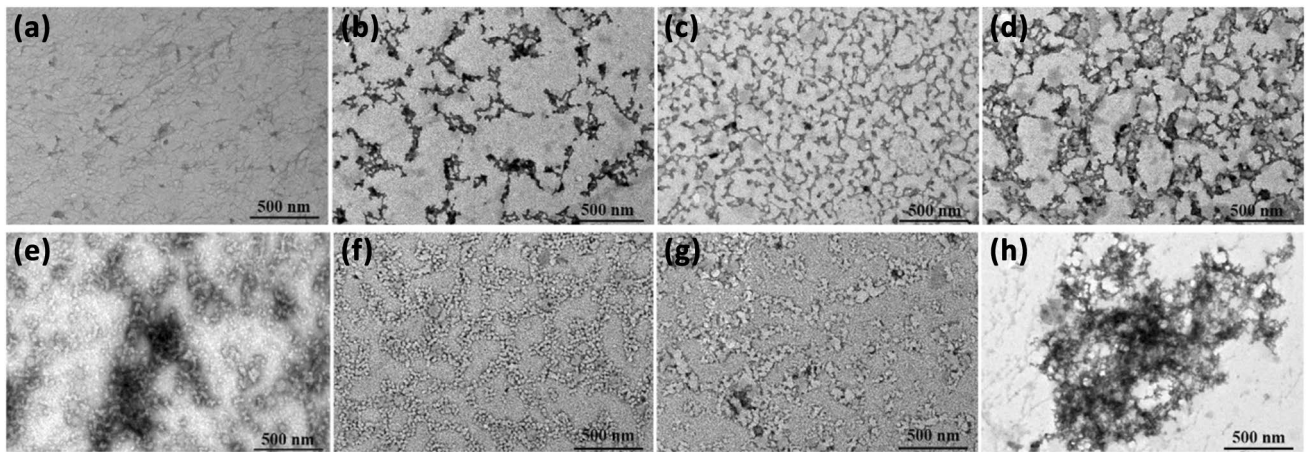
Fig. 5 Transmission electron micrographs of candy and fresh abalones under different simmering times. **a–d** Candy abalone simmered for 0, 5, 7.5 and 10 h. **e–h** Fresh abalone simmered for 0, 5, 7.5 and 10 h

glycolysis, protein kinases, phosphorylases, transferases and cytochrome C. Salt-soluble proteins are based on myofibrillar proteins, which consist of thick and thin filaments. The thick filaments include myosin and paramyosin, and the thin filaments contain actin, tropomyosin and troponin.

The changes in each protein fraction during the simmering process of dried and fresh abalones are shown in Fig. 6a, b and c. In the electrophoretograms of water-soluble and salt-soluble proteins (Fig. 6a and b), the number and intensity of protein bands of fresh abalone gradually decreased as the simmering time increased. However, in the insoluble protein electrophoretogram (Fig. 6c), the fresh abalone had more kinds of proteins with higher content. This indicates that the water-soluble proteins and salt-soluble proteins of fresh abalone were denatured and crosslinked into a gel during simmering. However, in figures a and b, little protein banding was seen throughout the simmering process of candy abalone, speculating whether the proteins were

denatured and crosslinked together after simmering like fresh abalone and thus in insoluble proteins. However, in Fig. 6c, it was found that there were no visible bands in the candy abalone sample, suggesting that peptides rather than intact proteins formed the crosslinking in the candy abalone gel.

The rheological characteristics of the peptides from candy abalone at different simmering times and concentrations

The rheological behavior of hydrogels can reflect their physical properties. We conducted an in vitro heating experiment to simulate the gel formation process to further investigate the self-assembly ability of peptides derived from dried abalone. Crude protein (w: $v = 1$: 2) was obtained by homogenizing candy and fresh abalones with cold deionized water respectively, to investigate the changes in storage modulus
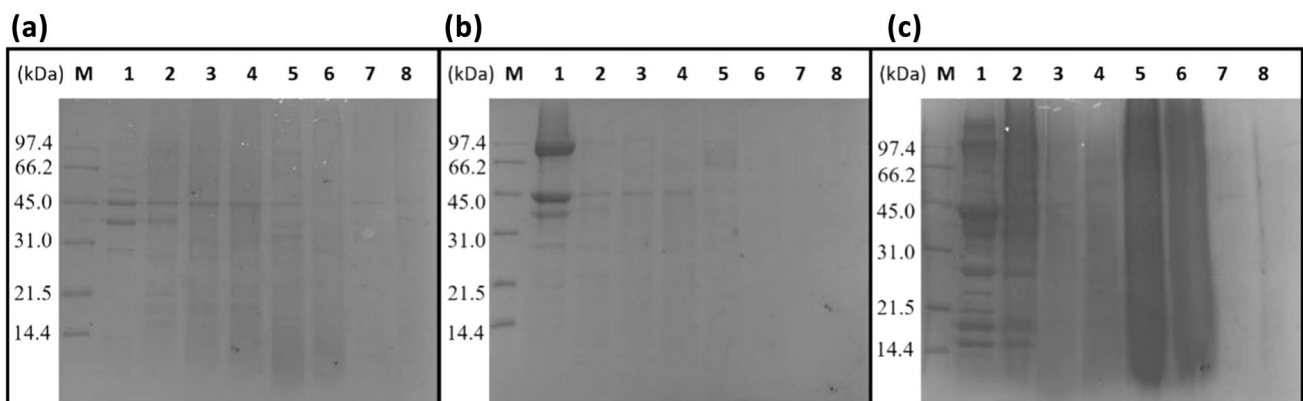

Fig. 6 SDS-PAGE analyses of **a** Water-soluble proteins, **b** Salt-soluble proteins, and **c** Precipitate. Lane M, protein markers and their corresponding molecular masses. Lane 1–4, the 0, 5, 7.5 and 10 h of fresh abalone. Lane 5–8, the 0, 5, 7.5 and 10 h of candy abalone

(G′) and loss modulus (G″) under different simmering times. It can be observed from Fig. 7a that at low strain, the crude protein gel of candy abalone was in the linear viscoelastic region, and the modulus remained constant. With the gradually increasing strain, the storage modulus and loss modulus gradually decreased in the nonlinear viscoelastic region. In the linear viscoelastic region, the storage modulus of the candy abalone gel was larger than the loss modulus, indicating its elastic dominant behavior and solid-like nature. However, above the critical strain value, both the storage modulus and loss modulus started to decrease, but the storage modulus was smaller than the loss modulus (G′ < G″), implying that the hydrogels had a shearing-thinning property and transformed to the solution state. Figure 7b demonstrated the variation of the loss factor of candy abalone peptide gels with heating time at this concentration. In the range of 0.1%-10% small strain, the loss factor remained stable with the increase of strain. As the degree of strain increased, the loss factor increased sharply, which indicated an increase in the energy dissipation of the peptide gel, a weakening of the solid-like properties, and a shortening of the lifetime of the bonds in the gel network. And the loss factor increased when the simmering time from 40 to 120 min, showing an increase in their viscosity. Therefore, its assembly capacity gradually improved. Overall, the rigidity and adhesiveness of candy abalone gel were higher than that of fresh abalone gel (Fig. S2a). Fig. S2b shows the variation of storage modulus and loss modulus of the mixture of crude protein and peptides from dried abalone at different concentrations heated for 120 min. It can be seen that the storage modulus and loss modulus of candy abalone gel increased significantly with increasing concentration, which was approximately 17.0 times the initial value. The rheological tests showed that the modulus of candy abalone gel was related to the simmering

time and concentration, and the concentration had a significant influence on it. Consistent with our result, Kim et al. found that silk fibroin can result in a hydrogel with higher compressive strength and modulus at a higher concentration [35]. Furthermore, the G″ can increase as the concentration of sunflower protein hydrolysate increases from 1.7 to 2.5% in the oscillatory mode [36].

Identification of possible peptides in candy abalone hydrogel and MD simulation analysis for the typical peptide

The possible peptides that formed the candy abalone hydrogel were detected by mass spectrometry, shown in Table S1. According to the results, about fifteen peptides were mainly involved in forming the candy abalone gel. Nine peptides, sharing similar amino acid sequences, were derived from paramyosin and had the highest score of 4789, more than ten times higher than other identified peptides from actin and myosin. Figure 8 shows the secondary mass spectra of the typical peptide derived from paramyosin (RKAQQLIEEADHRADMAEKNLVAVR), which is highlighted in the amino acid sequence of paramyosin. Furthermore, the distribution of amino acid residues on the outer surface of abalone paramyosin has been analyzed. It was found that the His and Glu residues located at positions i, i+4 were distributed through the α-helix. Three amino acid residues formed a helix between His-Glu, which allowed the side chains of His and Glu residues to be exposed in the same direction on the α-helix [20]. Thus, if the appropriate conditions were provided, such as zinc ions, self-assembly of abalone paramyosin into hydrogels was induced. Suzuki et al.[37] reported that paramyosin in abalone was relatively unstable under heat treatment and disappeared after 10 min
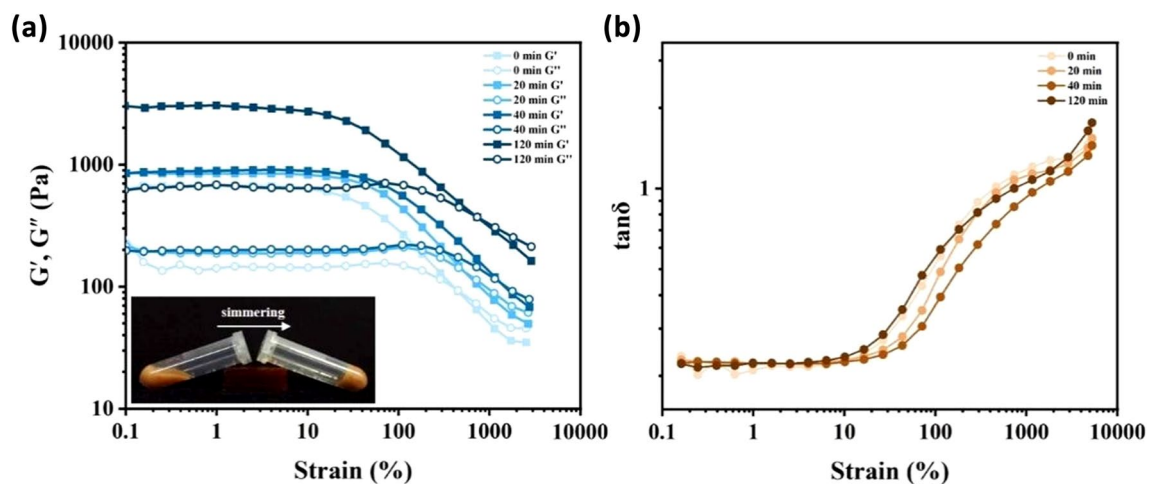

Fig. 7 Strain-dependent oscillatory shear rheology of the peptide hydrogel from candy abalone at different simmering times with a fixed frequency of 1 Hz at 25.0 ± 0.1 °C
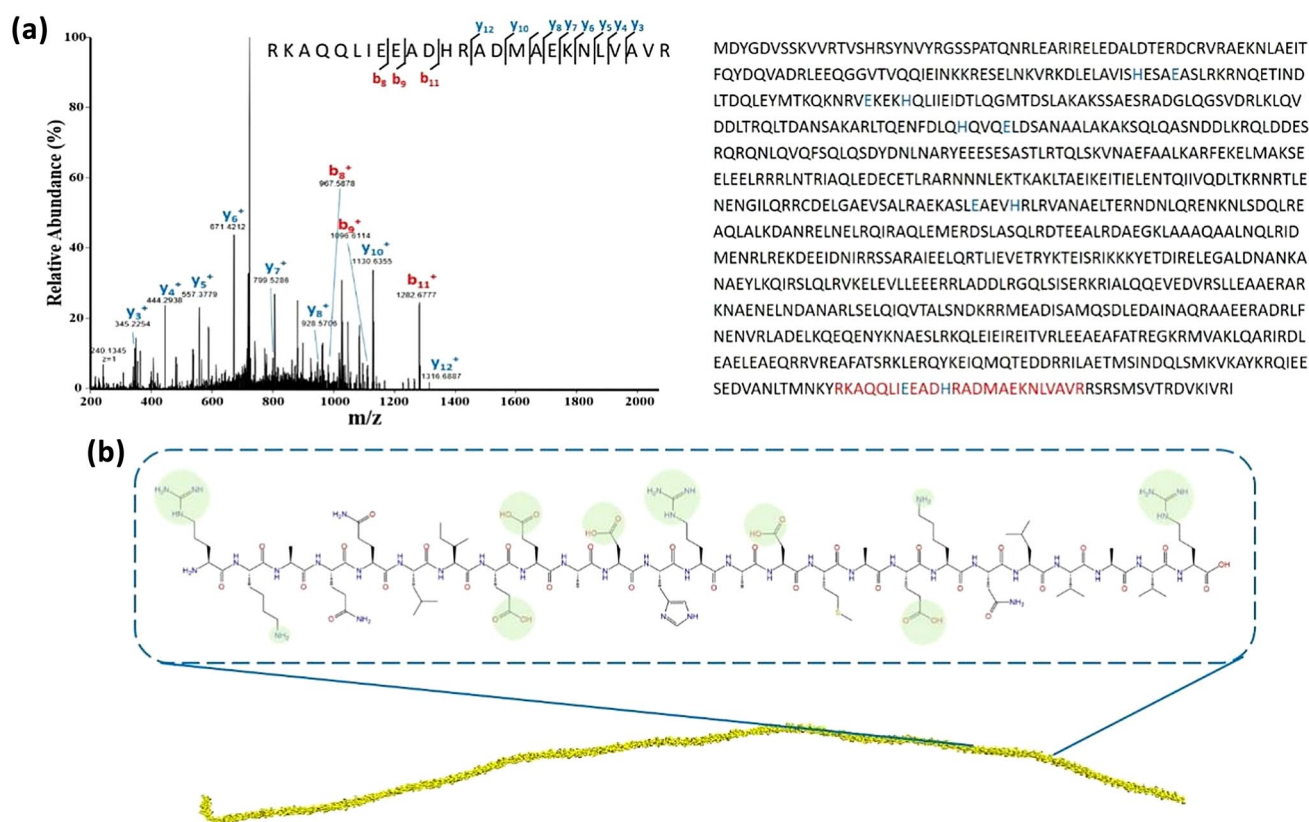
Fig. 8 Secondary mass spectra of **a** a typical paramyosin-derived peptide and **b** its two-dimensional structure and three-dimensional structure of paramyosin subunit predicted by trRosetta

of heating in boiling water. Therefore, paramyosin is closely related to the changes in properties of dried abalone gel during simmering.

In order to further investigate the formation possibility and process of candy abalone hydrogel, we used molecular dynamics simulation to study the self-assembly of the typical peptide from paramyosin. In the molecular dynamics study, we evaluated the system using the root mean square deviation (RMSD), the radius of gyration (Rg), solvent accessible surface area (SASA) and the results are shown in Fig. 9 and Fig. S3. The RMSD of the molecular dynamics simulated protein backbone is shown in Fig. 9a. The result indicated that the RMSD of the whole simulated system remains stable after 220 ns with fluctuations less than 0.1 nm, which illustrated that the whole simulated system had reached equilibrium [38]. The result of the radius of gyration for peptide self-assembly is displayed in Fig. S3a. The result showed that Rg decreased, indicating that the whole system was more compact and had better stability [39]. The SASA (Fig. S3b) also showed that the system was more stable with a longer simulation time. The above results were then analyzed using the Free Energy Landscape (FEL), and shown in Fig. S3c. Only one energy minimum in the FEL during the 250 ns molecular dynamics simulation stated that a stable

conformation existed for the peptide self-assembly. In combination with the FEL result, dihedral angle analysis was performed, and a Ramachandran plot was generated. The results showed (Fig. 9b) that 95% of the amino acid residues fell within the allowed and maximum allowed regions, suggesting that the conformation of the model conformed to the rules of stereochemistry and could be used for subsequent analysis. Subsequently, the number of hydrogen bonds was counted and gradually increased during the self-assembly of the polypeptides, showing that hydrogen bonds had a positive effect on the formation of the structure (Fig. S3d). Finally, the force analysis of the hydrogen bonds surface and the charged surface of the self-assembled peptides revealed that hydrogen bonds mainly mediated the self-assembly of the peptides during the rehydration phase and hydrophobic interactions with partial involvement of electrostatic interactions during the simmering stage (Fig. 9c, d and Fig. S3e).

Specific carboxyl, guanidyl, and amino groups in Glu, Asp, Arg, and Lys readily form hydrogen bonds [40]. These amino acids account for approximately 28, 24 and 21% of the total amino acids in peptides derived from paramyosin, actin, and myosin heavy chain (fragment), respectively. This facilitates the self-assembly of dry abalone peptides. Amphiphilic peptides presented
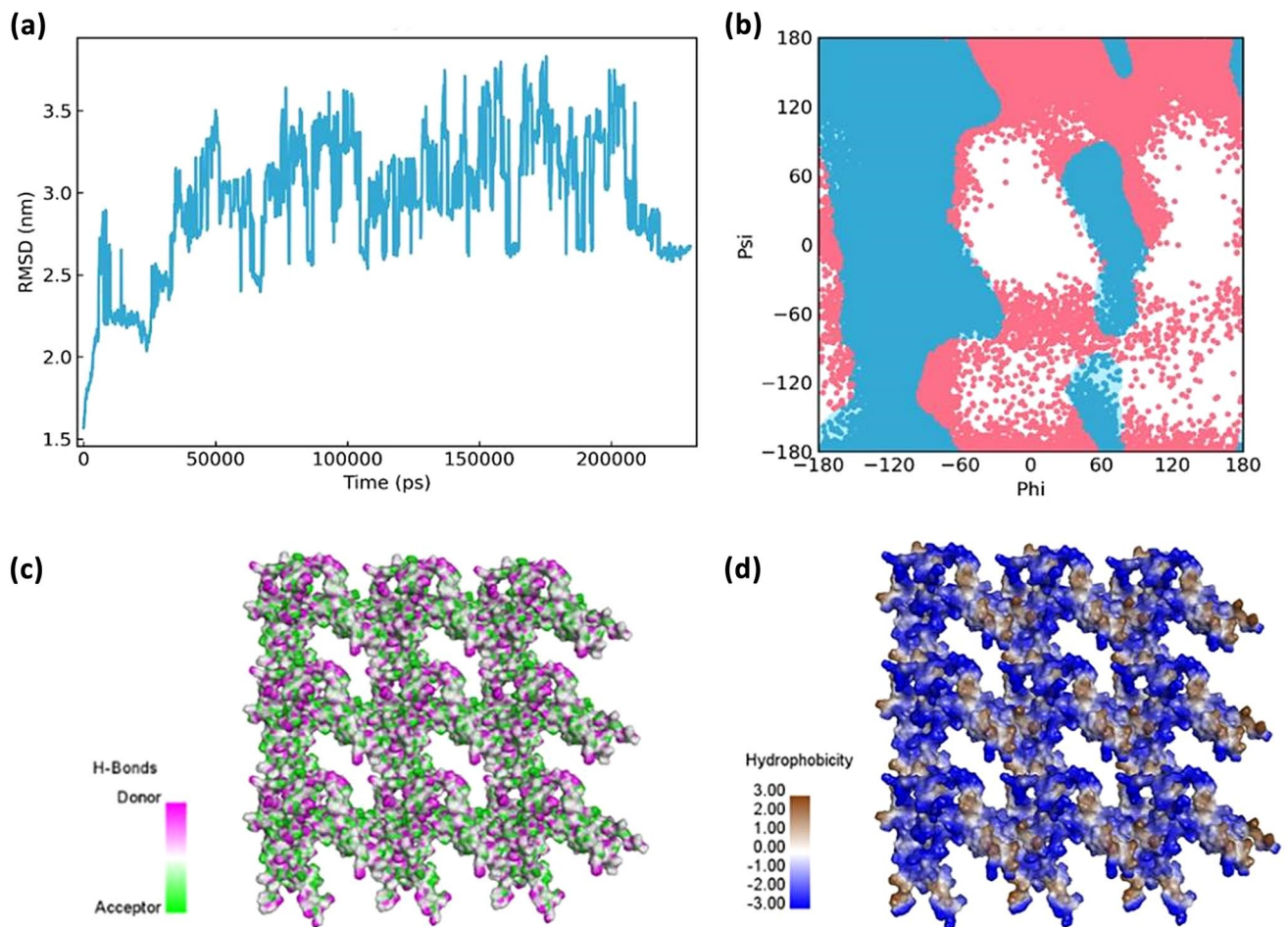
(a)

(b)

(c)

(d)

Fig. 9 Molecular dynamics results of the self-assembly of peptides. **a** RMSD, **b** Ramachandran plot, **c** Hydrogen bonds, and **d** Hydrophobic interactions

alternating hydrophobic (X) and hydrophilic (Z) residues, called (XZXZ)n sequence, and had a strong ability to self-assemble into hydrogels by hydrophobic aggregation [41]. In the possible peptide sequences that form the candy abalone, hydrophobic and hydrophilic amino acids alternate, accounting for approximately 50% of the total amino acids. This explains that the formation of candy abalone hydrogel in molecular dynamics simulation is mainly due to hydrogen bonding and hydrophobic interactions. Moreover, amino acids with high helicity in these peptides, especially Leu and Ala, can improve the stability of the three-dimensional network structure of peptide hydrogels [42]. In addition, the hydroxyl group of glutamic acid promotes peptide chain interactions through hydrogen bonding. The guanidine side chain of arginine increases peptide-peptide interactions through hydrogen bonding and electrostatic interactions, which influence the network topology and the mechanical properties of the hydrogels [43]. These results suggest that the composition and sequence of amino acids in dried abalone peptides conform to the rules of peptide

self-assembly to form hydrogels, which also explain the formation mechanism of the viscoelastic candy abalone.

In food hydrogels, the 3D network superstructures are commonly constructed by cross-linking protein filaments at branch point linkages. Paramyosin is a high-ordered thick filament that widely exists within invertebrate muscles. It exhibits a coiled-coil structure, thus interacting with each other to form hydrogels under some conditions. In our previous work, metal ions and organic molecules can participate in cross-linking, strengthening the mechanical property [20, 44]. While when the filamentous protein degraded during processing, the mechanical, rheological, and morphological properties of paramyosin peptides have significant changes. A few reasons may contribute to the results. Firstly, the side chains were totally exposed, leading to more chances to form a network. Moreover, the loss factor of the candy abalone gel was greater than fresh abalone gel after 10 h simmering in the linear viscoelastic range (Table 1). This may also be a key factor in why the candy-like core is more viscous. Secondly, the control of peptide gelation is multi-dimensional,

which is not so stable as coiled-coil interactions existed between paramyosins. This may be the reason of easily gel-sol transition of candy abalone.

Conclusions

This study found that myofibrillar protein in the adductor muscle of dried abalone could form a dense three-dimensional network hydrogel structure. The formation of such a hydrogel structure might be derived from the degradation of the myofibrillar protein during the drying process. By using the mass spectrometry, we identified degraded peptides in candy abalone, which mainly stemmed from paramyosin. Moreover, molecular dynamics simulation revealed that these peptides possessed self-assembly properties, leading to the formation of the hydrogel through hydrogen bonds and hydrophobic interactions during the rehydration and simmering stages, thereby producing a unique viscoelastic adductor in the candy abalone. This study revealed the mechanism of the formation of candy abalone that the production of peptide hydrogel contributed to the tender and viscoelastic textural property of candy abalone.

Data availability The authors declare that the data supporting the findings of this study are available within the paper and the supplementary information file. If raw data files are needed, they are available from the corresponding author upon reasonable request.

Declarations

Conflict of interest The authors have no competing interests to declare that are relevant to the content of this article.

Research involving human and animal participants This article does not contain any studies with human participants or animal subjects.

References

1. Suleria HAR, Masci PP, Gobe GC, Osborne SA (2017) Therapeutic potential of abalone and status of bioactive molecules: a comprehensive review. Crit Rev Food Sci Nutr 57:1742–1748
2. Venugopal V, Gopakumar K (2017) Shellfish: nutritive value, health benefits, and consumer safety. Compr Rev Food Sci Food Saf 16:1219–1242
3. Shi L, Hao G, Chen J, Ma S, Weng W (2020) Nutritional evaluation of Japanese abalone (*haliotis discus hannai Ino*) muscle: Mineral content, amino acid profile and protein digestibility. Food Res Int 129:108876
4. Hassoun A, Çoban ÖE (2017) Essential oils for antimicrobial and antioxidant applications in fish and other seafood products. Trends Food Sci Technol 68:26–36
5. Porturas OR, Ushio H, Watabe S, Takada K, Hatae K (1993) Toughness and collagen content of abalone muscles. Biosci Biotechnol Biochem 57:6–11
6. Tornberg EVA (2005) Effects of heat on meat proteins-implications on structure and quality of meat products. Meat Sci 70:493–508
7. Hughes JM, Oiseth SK, Purslow PP, Warner RD (2014) A structural approach to understanding the interactions between colour, water-holding capacity and tenderness. Meat Sci 98:520–532
8. Pathare PB, Roskilly AP (2016) Quality and energy evaluation in meat cooking. Food Eng Rev 8:435–447
9. Yin L, Zhou F, Yao L, Wang X (2020) Protein distribution characteristics in different muscle parts of *haliotis discus hannai*. Sci Technol Food Ind 41:93–98
10. Szent- Györgyi AG, Cohen C, Kendrick-Jones J (1971) Paramyosin and the filaments of molluscan "catch" muscles. J Mol Biol 56:239–258
11. Watabe S, Kantha SS, Hashimoto K, Kagawa H (1990) Phosphorylation and immunological cross-reactivity of paramyosin: a comparative study. Comp Biochem Physiol 96:81–88
12. Watabe S, Iwasaki K, Funabara D, Hirayama Y, Nakaya M, Kikuchi K (2000) Complete amino acid sequence of *mytilus* anterior byssus retractor paramyosin and its putative phosphorylation site. J Exp Zool 286:24–35
13. Park D, Xiong YL (2007) Oxidative modification of amino acids in porcine myofibrillar protein isolates exposed to three oxidizing systems. Food Chem 103:607–616
14. Smuder AJ, Kavazis AN, Hudson MB, Nelson WB, Powers SK (2010) Oxidation enhances myofibrillar protein degradation via calpain and caspase-3. Free Radic Biol Med 49:1152–1160
15. Xue M, Huang F, Huang M, Zhou G (2012) Influence of oxidation on myofibrillar proteins degradation from bovine via μ-calpain. Food Chem 134:106–112
16. Sun XD, Holley RA (2011) Factors influencing gel formation by myofibrillar proteins in muscle foods. Compr Rev Food Sci Food Saf 10:33–35
17. Truong BQ, Buckow R, Nguyen MH, Furst J (2017) Gelation of barramundi (*Latesz calcarifer*) minced muscle as affected by pressure and thermal treatments at low salt concentration. J Sci Food Agric 97:3781–3789
18. Yang Y, Liu X, Xue Y, Xue C, Zhao Y (2020) The process of heat-induced gelation in *Litopenaeus vannamei*. Food Hydrocoll 98:105260
19. Le H, Ting L, Jun C, Weng W (2018) Gelling properties of myofibrillar protein from abalone (*haliotis discus hannai ino*) muscle. Int J Food Prop 21:277–288
20. Chen X, Liu Y, Yin S, Zang J, Zhang T, Lv C, Zhao G (2022) Construction of sol-gel phase-reversible hydrogels with tunable properties with native nanofibrous protein as building blocks. ACS Appl Mater Interfaces 14:44125–44135
21. Zhu S, Luo Y, Hong H, Feng L, Shen H (2013) Correlation between electrical conductivity of the gutted fish body and the quality of bighead carp (*Aristichthys nobilis*) heads stored at 0 and 3 C. Food Bioprocess Technol 6:3068–3075
22. Urbonaite V, De Jongh HHJ, Van Der Linden E, Pouvreau L (2015) Water holding of soy protein gels is set by coarseness, modulated by calcium binding, rather than gel stiffness. Food Hydrocoll 46:103–111
23. Tadpitchayangkoon P, Park JW, Mayer SG, Yongsawatdigul J (2010) Structural changes and dynamic rheological properties of sarcoplasmic proteins subjected to pH-shift method. J Agric Food Chem 58:4241–4249

24. Laemmli UK (1970) Cleavage of structural proteins during the assembly of the head of bacteriophage T4. Nature 227:680–685

25. Øiseth SK, Delahunty C, Cochet M, Lundin L (2013) Why is abalone so chewy? structural characterization and relationship to textural attributes. J Shellfish Res 32:73–79

26. Ganhão R, Morcuende D, Estévez M (2010) Protein oxidation in emulsified cooked burger patties with added fruit extracts: Influence on colour and texture deterioration during chill storage. Meat Sci 85:402–409

27. Pons M, Fiszman SM (1996) Instrumental texture profile analysis with particular reference to gelled systems. J Texture Stud 27:597–624

28. Herrero AM, Cambero MI, Ordóñez JA, De la Hoz L, Carmona P (2008) Raman spectroscopy study of the structural effect of microbial transglutaminase on meat systems and its relationship with textural characteristics. Food Chem 109:25–32

29. Delbarre-Ladrat C, Chéret R, Taylor R, Verrez-Bagnis V (2006) Trends in postmortem aging in fish: understanding of proteolysis and disorganization of the myofibrillar structure. Crit Rev Food Sci Nutr 46:409–421

30. Yan C, Pochan DJ (2010) Rheological properties of peptide-based hydrogels for biomedical and other applications. Chem Soc Rev 39:3528–3540

31. Taherian AR, Mondor M, Labranche J, Drolet H, Ippersiel D, Lamarche F (2011) Comparative study of functional properties of commercial and membrane processed yellow pea protein isolates. Food Res Int 44:2505–2514

32. Renkema JMS, Vliet TV (2002) Heat-induced gel formation by soy proteins at neutral pH. J Agric Food Chem 50:1569–1573

33. Borderías AJ, Tovar CA, Domínguez-Timón F, Díaz MT, Pedrosa MM, Moreno HM (2020) Characterization of healthier mixed surimi gels obtained through partial substitution of myofibrillar proteins by pea protein isolates. Food Hydrocoll 107:105976

34. Kocher PN, Foegeding EA (1993) Microcentrifuge-based method for measuring water-holding of protein gels. J Food Sci 58:1040–1046

35. Kim UJ, Park J, Li C, Jin HJ, Valluzzi R, Kaplan DL (2004) Structure and properties of silk hydrogels. Biomacromol 5:786–792

36. Sanchez AC, Burgos J (1997) Gelation of sunflower globulin hydrolysates: rheological and calorimetric studies. J Agric Food Chem 45:2407–2412

37. Suzuki M, Kobayashi Y, Hiraki Y, Nakata H, Shiomi K (2011) Paramyosin of the disc abalone *haliotis discus*: identification as a new allergen and cross-reactivity with tropomyosin. Food Chem 124:921–926

38. Qiu Y, Liu Q, Tu G, Yao XJ (2022) Discovery of the cryptic sites of SARS-CoV-2 papain-like protease and analysis of its druggability. Int J Mol Sci 23:11265

39. Li X, Guo J, Lian J, Gao F, Khan AJ, Wang T, Zhang F (2021) Molecular simulation study on the interaction between tyrosinase and flavonoids from sea buckthorn. ACS Omega 6:21579–21585

40. Yu M, Lin S, Ge R, Xiong C, Xu L, Zhao M, Fan J (2022) Buckwheat self-assembling peptide-based hydrogel: Preparation, characteristics and forming mechanism. Food Hydrocoll 125:107378

41. Bowerman CJ, Nilsson BL (2012) Review self-assembly of amphipathic β-sheet peptides: insights and applications. Pept Sci 98:169–184

42. Fu K, Wu H, Su Z (2021) Self-assembling peptide-based hydrogels: fabrication, properties, and applications. Biotechnol Adv 49:107752

43. Gao J, Tang C, Elsawy MA, Smith AM, Miller AF, Saiani A (2017) Controlling self-assembling peptide hydrogel properties through network topology. Biomacromol 18:826–834

44. Yin S, Duan M, Qian Y, Lv C, Zang J, Zhao G, Zhang T (2023) Regulatable and reversible native paramyosin hydrogels promote the wound healing of the skin in mice. Chem Eng J 462:142294